Journal of Organometallic Chemistry, 366 (1989) 391–401
Elsevier Sequoia S.A., Lausanne – Printed in The Netherlands
JOM 09780

Reactions of the rhodium dihydride complex $[RhH_2(Hex\text{-}DAB)(PPh_3)_2][PF_6]$ (cHex-DAB = $C_6H_{11}N{=}CHCH{=}NC_6H_{11}$) with $[PPh_4][Co(CO)_4]$ and $[PPh_4][HFe(CO)_4]$. The crystal structure of $[RhH_2(cHex\text{-}DAB)(PPh_3)_2][Co(CO)_4]$

Marta Iglesias, Carmen del Pino, Ana San José

Instituto de Ciencia de Materiales de Madrid, Sede D, CSIC, Serrano 113, 28006 Madrid (Spain)

Sagrario Martínez-Carrera

Instituto Rocasolao, CSIC, Serrano 117, 28006 Madrid (Spain)

and Josep Ros *

Departament de Química, A-10, Universitat Autònoma de Barcelona, 08193 Bellaterra (Spain)

(Received October 28th, 1988)

Abstract

The dihydride complex $[RhH_2(cHex\text{-}DAB)(PPh_3)_2][PF_6]$ reacts with $[PPh_4][Co(CO)_4]$ and $[PPh_4][HFe(CO)_4]$ to give the ionic complexes $[RhH_2(cHex\text{-}DAB)(PPh_3)_2][Co(CO)_4]$ and $[Rh(cHex\text{-}DAB)(PPh_3)_2][HFe(CO)_4]$ and neutral mixed Rh/Co and Rh/Fe complexes containing bridging cHex-DAB ligands and metal–metal bonds. The complex $[RhH_2(cHex\text{-}DAB)(PPh_3)_2][Co(CO)_4]$ was studied by X-ray crystallography and shown to consist of cations $[RhH_2(cHex\text{-}DAB)(PPh_3)_2]^+$ and anions $[Co(CO)_4]^-$ linked by coulombic forces, and possibly hydrogen bonds between the imine hydrogens and the oxygens of the carbonyl ligands.

Introduction

1,4-Diazadienes have been widely used as bridging ligands between two different metals, and found to exhibit two possible modes of coordination, σ-N, μ-N′, η^2-C=N′ and η^2 = -C=N, η^2-C′=N′ [1]. These ligands can also be converted by metallic hydrides into 3-amino-1-aza-allyl coordinated fragments bonded to two metallic centres [2]. We are engaged in a systematic study of diazabutadienes and here investigated the synthesis and the reactions of cationic rhodium *cis*-dihydride complexes containing diazabutadiene and phosphine ligands [3]. Cyclooligomeriza-

0022-328X/89/$03.50

tion of acetylenes was observed and some metallacyclopentadiene intermediates were also isolated [4] in these reactions. The cationic nature of rhodium complexes raises the possibility of interesting reactions with anionic carbonyl complexes, permitting exploration of new aspects of the behaviour of R-DAB as bridging ligands [5]. Such reactions should give heterodinuclear complexes on Rh-DAB species increasing the range of heterometallic compounds bridged by nitrogen ligands [6,7]. The rhodium complexes are very active catalysts, and so interesting possibilities can be expected when other metals are incorporated. An example of enhancement of catalysis by a second metal in a heterobinuclear complex containing a nitrogen centred bridging ligand has recently been reported [8]. We describe below the reactions of $[RhH_2(cHex\text{-}DAB)(PPh_3)_2]^+$ (cHex-DAB = $C_6H_{11}N{=}CHCH{=}NC_6H_{11}$) with $[Co(CO)_4]^-$ and $[HFe(CO)_4]^-$ to give heterobimetallic complexes containing various types of DAB bridges.

Results and discussion

The reactions of $[RhH_2(cHex\text{-}DAB)(PPh_3)_2][PF_6]$ (cHex-DAB = $C_6H_{11}N{=}CH\text{-}CH{=}NC_6H_{11}$) with the carbonyl complexes $[PPh_4][Co(CO)_4]$ and $[PPh_4][HFe(CO)_4]$ at room temperature and in CH_2Cl_2 solutions were found to give red-brown solutions containing new mixed Rh–Co and Rh–Fe complexes contaminated by carbonyl-chloro-triphenylphosphine complexes of rhodium, which were removed by precipitation of $[PPh_4][PF_6]$ with diethyl ether and concentration on a vacuum line. The first precipitate contained a mixture of $[RhCl(CO)(PPh_3)_2]$ and $[Rh_2Cl_2(CO)(PPh_3)_3]$ which were identified by comparison of their spectroscopic data with those in the literature [9]. Spectroscopic data for the products are given in Table 1.

Reactions with $[Co(CO)_4]^-$

When stoichiometric amounts of $[RhH_2(cHex\text{-}DAB)(PPh_3)_2][PF_6]$ (cHex-DAB = $C_6H_{11}N{=}CHCH{=}NC_6H_{11}$) and $[PPh_4][Co(CO)_4]$ was dissolved and mixed in CH_2Cl_2 at room temperature the complex $[RhH_2(cHex\text{-}DAB)(PPh_3)_2][Co(CO)_4]$ (**1**) was isolated after precipitation of $[PPh_4][PF_6]$ in diethyl ether. The ^1H NMR spectrum of **1** was identical to that the starting cation, but the IR spectrum in KBr pellet in the $\nu(CO)$ region showed three bands, suggesting some distortion of the anion, and the presence of such distortion was confirmed by an X-ray diffraction study of complex **1**. When the same reaction was carried out in refluxing CH_2Cl_2, the complex of $[RhCo(CO)_4(cHex\text{-}DAB)(PPh_3)]$ (**3**) was formed. The ^1H NMR spectrum of **3** showed imine signals at 7.91 and 3.71 ppm characteristic of a σ-N,μ-N′,η^2-C=N′,cHex-DAB ligand. A broad signal at 7.5 ppm which integrated as 15 H indicated the presence of a single PPh_3 ligand in the molecule. The IR spectrum of **3** shows four intense bands between 1945 and 1870 cm^{-1} corresponding to terminal carbonyl ligands. The complex **3** seems to be formed by a thermal rearrangement of **1** after elimination of H_2 and PPh_3. The presence of a metal–metal bond in **3** is indicated by electron counting.

Molecular structure of $[RhH_2(C_6H_{11}N{=}CHCH{=}NC_6H_{11})(P(C_6H_5)_3)_2][Co(CO)_4]$ (1)

The molecular structure of **1** is shown in the Fig. 1. Atom coordinates are given in Table 2 and some relevant bond lengths and bond angles in Table 3.

Table 1

IR [a] and ^1H NMR [b] data for products

Compound	ν(CO) region (cm^{-1})	^1H NMR (ppm) for different groups			
		Imino	cHex	PPh_2	Hydride
$[RhH_2(cHex\text{-}DAB)(PPh_3)_2][Co(CO)_4]$ **(1)**	2040 m (Ru–H) 2000m 1955 m 1875 vs	8.35 (s,2H)	2.76 (t,2H) 1.25–0.52 (m,20H)	7.61 (m,30H)	−15.67 (q,2H)
$[Rh(cHex\text{-}DAB)(PPh_3)_2][HFe(CO)_4]$ **(2)**	2047 m 1983 vs 1936 m	8.03 (s,2H)	1.50–0.85 (m,22H)	7.74–7.45 (m,30H)	
$[RhCo(CO)_4(cHex\text{-}DAB)(PPh_3)]$ **(3)**	1945 vs 1910 sh 1885 s 1870 s	7.91(s, 1H) 3.71 (d,1H)	3.15 (t,2H) 1.78–0.85 (m,20H)	7.72–7.40 (m,15H)	
$[RhFeH(CO)_4(cHex\text{-}DAB)(PPh_3)]$ **(4)**	2056 vs 1976 vs 1885 w 1789 m	8.27 (s,1H) 3.71 (d,1H)	2.19 (t,2H) 1.26–0.86 (m,20H)	7.70–7.40 (m,15H)	−15.63 (q,1H)
$[RhFe(CO)_4(cHex\text{-}DAB)(PPh_3)]$ **(5)**	2048 m 1971 vs 1829 w	7.8 (s,1H) 3.6 (d,1H)	2.0–0.88 (m,22H)	7.75–7.43 (m,15H)	
$[RhFeH(CO)_2(cHex\text{-}DAB)(PPh_3)_2]$ **(6)**	2042 m 1962 vs	7.92 (s,2H)	1.50–0.85 (m,22H)	7.74–7.45 (m,30H)	−15.7 (q,1H)

[a] In Kbr disks except for 4 (CH_2Cl_2). [b] Chemical shift (δ ppm) from TMS in $CDCl_3$.

Table 2

Atomic coordinates for the complex **1**

Atom	x	y	z	U_{eq}
Rh1	0.6259(1)	0.1044(1)	0.3014(1)	43(1)
Co1	0.4618(3)	0.3757(2)	0.2614(3)	65(2)
P1	0.5794(4)	0.0627(3)	0.1782(4)	38(2)
C111	0.6121(14)	0.1001(12)	0.0816(15)	41(9)
C112	0.5852(18)	0.1560(10)	0.0726(17)	47(10)
C113	0.6131(22)	0.1849(11)	0.0041(21)	75(13)
C114	0.6598(26)	0.1600(12)	−0.0592(24)	101(16)
C115	0.6904(23)	0.1042(15)	−0.0535(22)	101(15)
C116	0.6607(19)	0.0729(10)	0.0169(19)	60(11)
C121	0.4502(15)	0.0519(8)	0.1669(17)	37(9)
C122	0.3931(16)	0.0692(10)	0.0955(17)	42(10)
C123	0.2960(18)	0.0591(11)	0.0895(19)	53(11)
C124	0.2488(21)	0.0330(12)	0.1537(24)	69(13)
C125	0.3029(22)	0.0146(10)	0.2238(21)	68(13)
C126	0.3997(17)	0.0248(10)	0.2310(17)	52(10)
C131	0.6289(17)	−0.0062(10)	0.1639(15)	40(9)
C132	0.7221(22)	−0.0169(12)	0.1803(17)	72(13)
C133	0.7666(17)	−0.0681(15)	0.1686(19)	71(13)
C134	0.7050(30)	−0.1105(15)	0.1447(19)	91(17)
C135	0.6095(24)	−0.1028(12)	0.1258(18)	76(13)
C136	0.5728(16)	−0.0512(10)	0.1346(16)	46(10)
P2	0.6787(4)	0.1062(3)	0.4393(4)	45(2)
C211	0.5779(14)	0.1009(10)	0.5172(16)	36(8)
C212	0.5910(17)	0.1218(12)	0.5967(20)	59(12)
C213	0.5170(26)	0.1169(13)	0.6545(20)	86(16)
C214	0.4311(23)	0.0881(13)	0.6326(24)	76(14)
C215	0.4274(22)	0.0645(12)	0.5528(22)	69(13)
C216	0.5002(16)	0.0706(11)	0.4990(18)	52(10)
C221	0.7413(17)	0.1688(10)	0.4720(17)	50(10)
C222	0.6893(21)	0.2178(13)	0.4768(19)	72(14)
C223	0.7343(29)	0.2695(11)	0.5007(20)	97(17)
C224	0.8344(35)	0.2661(23)	0.5179(36)	150(0)
C225	0.8869(27)	0.2185(13)	0.5178(27)	103(19)
C226	0.8402(20)	0.1699(12)	0.4960(22)	73(13)
C231	0.7616(18)	0.0507(12)	0.4696(20)	51(11)
C232	0.7836(28)	0.0368(16)	0.5507(22)	109(19)
C233	0.8375(25)	−0.0067(18)	0.5784(23)	94(17)
C234	0.8815(21)	−0.0382(15)	0.5155(28)	79(15)
C235	0.8687(31)	−0.0259(18)	0.4303(27)	113(22)
C236	0.8091(22)	0.0194(13)	0.4099(20)	78(14)
N1	0.5104(13)	0.1659(8)	0.3112(12)	38(8)
C11	0.4083(17)	0.1582(9)	0.3370(19)	47(10)
C12	0.3859(19)	0.1919(13)	0.4173(20)	75(12)
C13	0.2802(21)	0.1793(14)	0.4425(26)	89(15)
C14	0.2050(19)	0.1888(15)	0.3815(27)	92(15)
C15	0.2243(22)	0.1590(16)	0.2977(27)	99(16)
C16	0.3378(22)	0.1729(14)	0.2656(23)	81(15)
C1	0.5401(18)	0.2144(12)	0.2908(18)	56(11)
C2	0.6466(20)	0.2230(14)	0.2664(20)	69(13)
N2	0.6976(13)	0.1783(9)	0.2659(14)	47(8)
C21	0.8129(32)	0.1807(13)	0.2522(26)	143(0)
C22	0.8354(37)	0.2375(24)	0.2477(57)	251(0)
C23	0.9696(27)	0.2317(19)	0.2352(43)	163(0)

Table 2 (continued)

Atom	x	y	z	U_{eq}
C24	0.9754(41)	0.2047(33)	0.1558(38)	241(0)
C25	0.9602(43)	0.1507(25)	0.1951(63)	311(1)
C26	0.8240(39)	0.1657(26)	0.1730(45)	200(0)
O1	0.5270(18)	0.3343(10)	0.4229(16)	120(12)
O2	0.2624(17)	0.3406(14)	0.2392(18)	144(15)
O3	0.5818(20)	0.3286(11)	0.1295(18)	122(13)
C3	0.5011(19)	0.3529(11)	0.3572(25)	82(14)
C4	0.5310(26)	0.3476(16)	0.1850(25)	99(17)
C5	0.3408(19)	0.3568(16)	0.2486(21)	85(15)
C6	0.4724(20)	0.4480(15)	0.2574(21)	71(13)
O4	0.4820(19)	0.4974(12)	0.2557(19)	127(13)

The molecular structure of **1** (Fig. 1) involves cations [RhH$_2$(C$_6$H$_{11}$N=CHCH=NC$_6$H$_{11}$)(P(C$_6$H$_5$)$_3$)$_2$]$^+$ and anions [Co(CO)$_4$]$^-$ complexes linked by coulombic intermolecular forces. The cations are mononuclear rhodium complexes with a distorted octahedral geometry containing two triphenylphosphine ligands, a C$_6$H$_{11}$N=CHCH=NC$_6$H$_{11}$ chelating ligand, and two hydrides. The phosphine ligands are pseudo-*trans* and tilted towards the hydride ligands, which were not located. The P(1)–Rh–P(2) angle is 152.5(3)°, the Rh(1)–P(1) and Rh(1)–P(2) distances are 2.094(67) and 2.063(6) Å; these lengths are shorter than those in other rhodium(III) complexes [10,11,12]. The cHex-DAB ligand and the rhodium lie almost in a plane, with Rh(1)–N(1) and Rh(1)–N(2) distances of 2.363(20) and 2.167(22) Å, respectively. The bond lengths and angles in the coordinated ligand are different from those in similar R-DAB rhodium(III) dihydride complexes; thus relative to that in the latter, the C(1)–C(2) distance of 1.742(43) Å is very large [11,12], as is the N(1)–Rh(1)–N(2) angle of 84.9(8)°. The anion [Co(CO)$_4$]$^-$ and the cations are packed in a way to minimize steric hindrance, but the carbonyl ligands are oriented towards the imine hydrogens in a way suggesting the possibility of hydrogen bonding. The shortest C–O distance is in the carbonyl ligand close to the cation but the large distortion of the tetrahedral geometry in the anion prevents confirmation of the presence of hydrogen bonding.

Reactions with [HFe(CO)$_4$]$^-$

The reaction of the complex [RhH$_2$(cHex-DAB)(PPh$_3$)$_2$][PF$_6$] with [PPh$_4$][HFe(CO)$_4$] is complex. At room temperature a mixture of compounds is always obtained, and depending on the reaction conditions various unambigously identified products can be isolated separatelly from the solution. Thus, when the reaction takes place in a CO atmosphere for about 2 h, an ionic complex **2** is obtained after precipitation of [PPh$_4$][PF$_6$] in diethyl ether. The IR spectrum of **2** in the ν(CO) region shows three bands characteristics of the anion [HFe(CO)$_4$]$^-$. The ^{1}H NMR spectrum of **2** is similar to the that of **1**, and similar to that of the starting cation [RhH$_2$(cHex-DAB)(PPh$_3$)$_2$]$^+$ except for the absence of the hydride signal at −15.6 ppm. These spectroscopic properties suggest an ionic nature for **2**: [Rh(cHex-DAB)(PPh$_3$)$_2$][HFe(CO)$_4$]. At room temperature under nitrogen, various products can be isolated by precipitation with diethyl ether depending on the reaction time. Thus, the products **4**, **5** and **6** are formed after 4 h , 24 h, and 4 days of reaction,

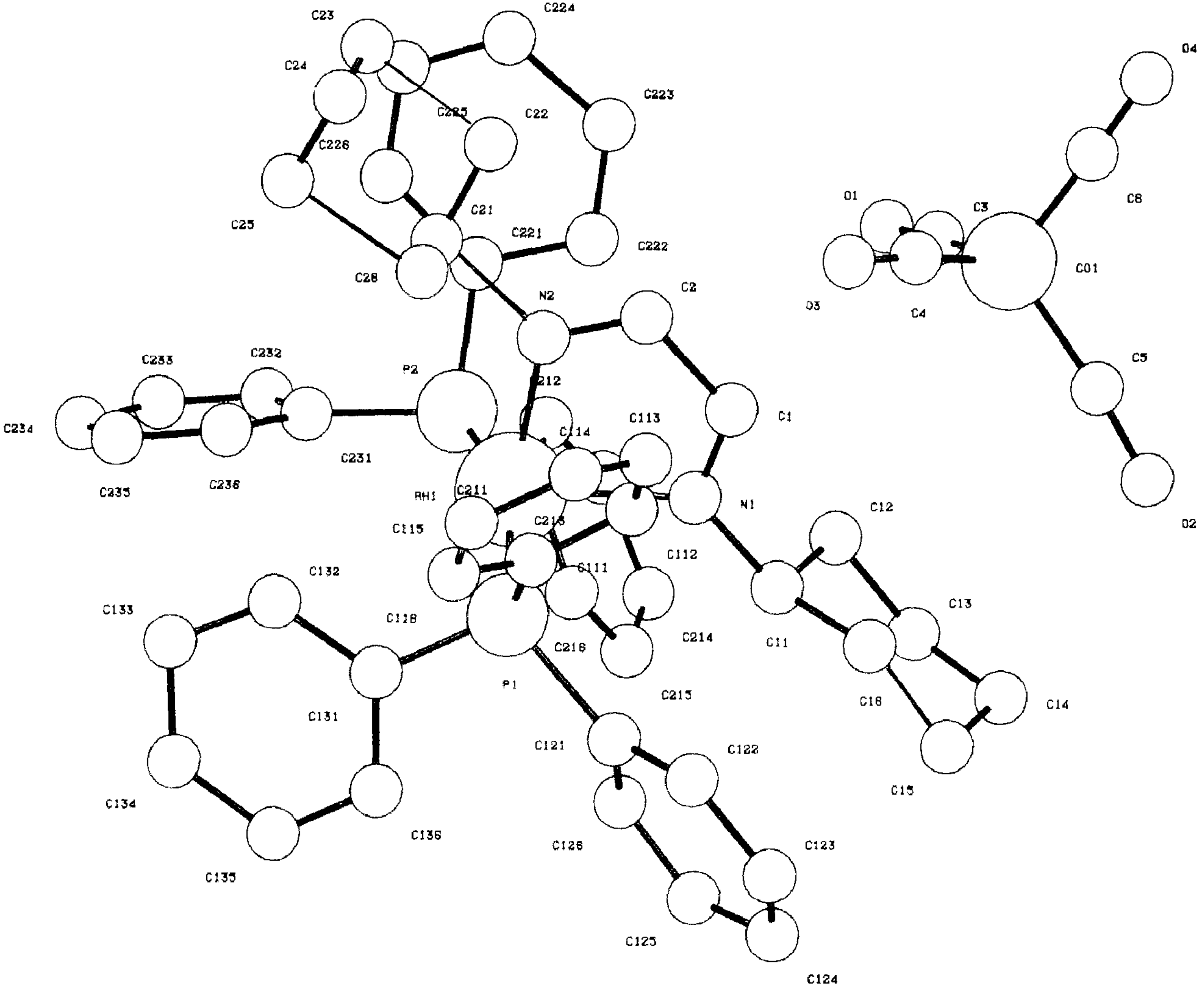

Fig. 1. The molecular structure of complex **1** showing the crystallographic numbering

Table 3

Selected bond lengths (Å) and angles (°) for complex **1**

Rh(1)-P(1)	2.094(6)	Rh(1)-P(2)	2.063(6)
Rh(1)-N(1)	2.363(20)	Rh(1)-N(2)	2.167(22)
Co(1)-C(3)	1.551(33)	Co(1)-C(4)	1.662(38)
Co(1)-C(5)	1.988(31)	Co(1)-C(6)	1.747(37)
P(1)-C(111)	1.680(24)	P(1)-C(121)	2.079(24)
P(1)-C(131)	1.844(25)	P(2)-C(211)	1.931(23)
P(2)-C(221)	1.859(26)	P(2)-C(231)	1.921(29)
N(1)-C(11)	1.675(34)	N(1)-C(1)	1.289(34)
N(2)-C(21)	1.847(55)	N(2)-C(2)	1.346(39)
C(1)-C(2)	1.742(43)	C(3)-O(1)	1.083(40)
C(4)-O(3)	1.200(47)	C(5)-O(2)	1.316(41)
C(6)-O(4)	1.197(46)		
Mean C-C distances in benzene rings	1.408(44)		
Mean C-C distances in cyclohexyl rings	1.475(57)		
N(1)-Rh(1)-N(2)	84.9(8)	N(2)-Rh(1)-P(1)	113.6(60
N(1)-Rh(1)-P(1)	94.0(5)	N(2)-Rh(1)-P(2)	88.4(6)
N(1)-Rh(1)-P(2)	113.6(6)	Rh(1)-N(1)-C(1)	106(2)
Rh(1)-N(2)-C(2)	107(2)	N(1)-C(1)-C(2)	120(2)
C(50-Co(1)-C(6)	108(2)	C(4)-Co(1)-C(6)	108(2)
C(4)-Co(1)-C(5)	119(2)	C(3)-Co(1)-C(6)	110(2)
C(3)-Co(1)-C(5)	113(2)	C(3)-Co(1)-C(4)	97(2)
Co(1)-C(3)-O(1)	176(2)	Co(1)-C(4)-O(3)	178(3)
Co(1)-C(5)-O(2)	176(3)	Co(1)-C(6)-O(4)	178(3)
P(1)-Rh(1)-P(2)	152.5(3)		
Mean (C-P-C)	107(1) °		
Mean (C-C-C) in benzene rings	120(3) °		
Mean (C-C-C) in cyclohexyl rings	110(3) °		

respectively. All of them are brown, microcrystalline products, soluble in CH_2Cl_2, and insoluble in petroleum ether and alcohols. The proposed structures for these complexes are shown in Scheme 1. It can be seen that two different modes of coordination of the cHex-DAB are present in the products. Complexes **4** and **5** contain a six electron bridging cHex-DAB, as could be concluded from their ^1H NMR spectra. The signals from the imine protons appear at 8.27 and 3.71 ppm for **4** and at 7.8 and 3.60 ppm for **5**. A quartet at -15.63 ppm is present in the ^1H NMR spectrum of **4**, corresponding to a hydride ligand linked to rhodium. The IR spectrum of **4** in the ν(CO) region shows one band of medium intensity, at 1780 cm^{-1} in a KBr pellet and at 1789 cm^{-1} in CH_2Cl_2 solution, that must be attributed to a bridging CO. Complex **5** shows only bands corresponding to terminal CO. Finally, the ^1H NMR spectrum, of complex **6** contains a signal at 7.92 ppm characteristic of a eight-electron bridging cHex-DAB and one at -15.7 ppm corresponding to a hydride ligand linked to rhodium. The presence of only terminal CO, ligands is indicated by the IR spectrum of **6**.

Complex **2** seems to represent the first step in the formation of complexes **4**, **5** and **6**, but **2** can only be isolated under a CO atmosphere after a reductive elimination of H_2 from the starting cation. Subsequently, the rhodium–iron bond is formed by coupling of the ions of **2**. The loss of different ligands generates the

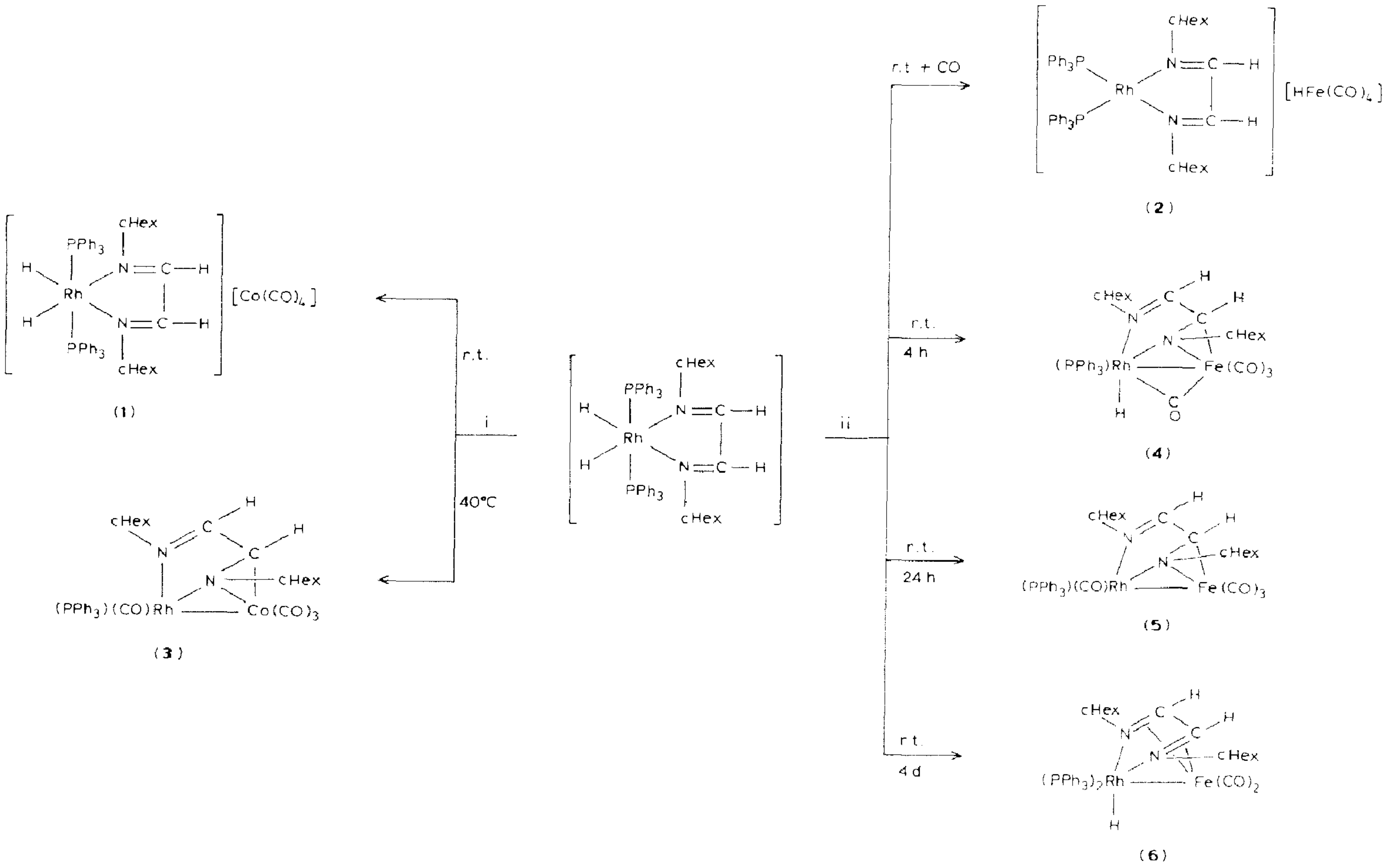

Scheme 1. i, $+ Co(CO)_4^-$; ii, $+ HFe(CO)_4^-$.

mixed complexes **4**, **5**, and **6**. No reasons can be offered for the formation of different complexes depending on the reduction time. No interconversions between the complexes have been detected. Determination of the molecular mass of the complexes by electronic impact mass spectrometry was not possible, and only the PPh_3 and cHex-DAB peaks were detected, which made more difficult the elucidation of the exact nature of the new complexes.

Experimental

All reactions were performed under N_2. The ^1H NMR spectra were recorded on a Bruker WM-360 Fourier spectrometer in $CDCl_3$ solution. Infrared spectra were recorded on a Nicolet 60SX (FT IS) spectrometer with KBr discs or CH_2Cl_2 solutions (ν(CO) region). Elemental analyses (C, H and N) were performed at Departamento de Química Inorgánica of the Universidad de Alcalá de Henares (Madrid). The qualitative presence of rhodium, cobalt and iron was determined by the X-ray fluorescence technique with a Philips PW 1540 apparatus with a tungsten anticathode.

The starting complexes $[RhH_2(C_6H_{11}N{=}CHCH{=}NC_6H_{11})(P(C_6H_5)_3)_2][PF_6]$ [3], $[PPh_4][Co(CO)_4]$ [13] and $[PPh_4][HFe(CO)_4]$ [14] were prepared by published procedures.

General procedure for the synthesis of products:

A slight excess of $[PPh_4][Co(CO)_4]$ or $[PPh_4][HFe(CO)_4]$ was added to a solution of $[RhH_2(cHex\text{-}dAB)(PPh_3)_2][PF_6]$ (0.25 g) in CH_2Cl_2 and the mixture was either stirred at room temperature or refluxed. Diethyl ether was then added and a white precipitate of $[PPh_4][PF_6]$ separated. The solid was filtered off and the solution concentrated, leading to separation of the carbonyl-chlorotriphenylphosphinerhodium complexes from the solution. Further concentration of the solution gave the mixed Rh/CO and Rh/Fe complexes, depending on the reaction condi-

Table 4

Elemental analyses, details of metals detected by X-ray fluorescence, and reaction conditions giving rise to specified product

Compound	Colour	Reaction conditions		X-ray fluorescence	Analyses: found (calc) (%)		
		time	temperature		C	H	N
1	orange-red	2 h	25 °C	Rh, Co	63.2 (63.5)	5.6 (5.5)	2.3 (2.7)
2	brown	2 h (CO)	25 °C	Rh, Fe	63.5 (63.8)	5.1 (5.4)	2.3 (2.8)
3	brown	2 h	40 °C	Rh, Co	57.0 (57.1)	5.3 (5.2)	3.1 (3.7)
4	brown	4 h	25 °C	Rh, Fe	57.1 (57.3)	5.6 (5.3)	3.1 (3.7)
5	brown	24 h	25 °C	Rh, Fe	57.5 (57.4)	4.9 (5.2)	3.0 (3.7)
6	brown	4 d	25 °C	Rh, Fe	64.8 (65.0)	5.3 (5.7)	2.1 (2.9)

tions. Table 4 lists the analytical data for products and shows the reaction conditions.

X-ray analysis of $[RhH_2(C_6H_{11}N{=}CHCH{=}NC_6H_{11})(P(C_6H_5)_3)_2][Co(CO)_4]$ *(1)*

The crystals used for the X-ray study were protected with paraffin oil to prevent decomposition, and sealed in Lindeman glass capillary tubes. Details of crystal data, data collection, and structure refinement are given in Table 5.

The rhodium atom was located from Patterson synthesis and the remaining non-hydrogen atoms by difference Fourier synthesis. Isotropic refinement was by full matrix least squares. An absorption correction [15] was then made, and the structure refined by full matrix least squares with anisotropic thermal parameters. The H atoms were located from successive difference maps and were kept fixed in

Table 5

Crystal data and details of data collection and structure refinement

Crystal data	
Formula	$C_{54}H_{51}N_2O_4CoRh$
Crystal habit	red, transparent prisms
Crystal size (mm)	$0.15 \times 0.20 \times 0.25$
Symmetry	Monoclinic, $P2_1/n$
Unit cell determination	least squares fit from 60 reflections
Unit cell dimensions (Å)	a 15.929(9), b 24.031(9), c 13.662(8) β 90.04(7)°
Packing: V (Å)^3, Z	5229.7(5), 4
D_c (gcm^{-3}), M, $F(000)$	1.21, 954.8, 1976
Experimental data	
Technique	Four circle diffractometer: Enraf–Nonius CAD-4. Bisecting geometry graphite-oriented monochromator: Mo-K_α, $\omega/2\theta$ scans, scan width: 1.5
Scanning range for	$2 < \theta < 30°$
Number of reflections:	
Measured	7529
Observed	2817
Standard reflections	2 reflections every 90 min, no variation I
Absorption coefficient μ	7.196 cm^{-1}
Solution and refinement [16]	
Solution mode	Patterson, Fourier and difference Fourier synthesis
Absorption correction [15]	applied after isotropic refinement
Refinement mode	least squares or F's, observed reflections only, anisotropic for non-hydrogen and isotropic for fixed H atoms.
Parameters: number of variables	535
w-scheme	empirical as to give no trends in $\langle w\, \Delta^2 F \rangle$ or $\langle \| F_o \| \rangle$ and $\langle \sin\theta/\lambda \rangle$ [17]
ΔF final	2.3 e Å^{-3} near Rh atom
Final R and R_w	0.090, 0.089
Computer and programs	VAX 11/750, XRAY 80 [16], DIFABS [15], PESOS [17], PARST [18]
Atomic factors	neutral atoms and anomalous dispersion-factors from International Tables for X-Ray Crystallography [19]

the refinement with isotropic thermal parameters corresponding to those of the atoms to which they were attached. R and R_w are defined as: $R = \Sigma|\Delta|/\Sigma|F_o|$ and $R_w = (\Sigma w^2/\Sigma w|F_o|^2)^{1/2}$ ($\Delta = |F_o| - |F_c|$).

Supplementary material available. Tables of thermal parameters, and calculated hydrogen positions, and structure factors are available from the authors.

Acknowlwedgements

We thank the C. I.C.Y.T. of Spain for financial support.

References

1 J. Keijsper, L.H. Polm, G. van Koten, K. Vrieze, E. Nielsen and C.H. Stam, Organometallics, 4 (1985) 2006.

2 J. Keijsper, J. Mul, G. van Koten, K. Vrieze, H.C. Ubbels and C.H. Stam, Organometallics, 3 (1984) 1732.

3 M. Iglesias, C. del Pino and J.L. Nieto, Inorg. Chim. Acta, 119 (1986) 7.

4 M. Iglesias, C. del Pino, J. Ros, S. García Blanco and S.M. Carrera, J. Organomet. Chem., 338 (1988) 89.

5 L.H. Staal, J. Keijpser, G. van Koten, K. Vrieze, J.A. Cras and W.P. Bosman, Inorg. Chem., 20 (1981) 555.

6 G. van Koten and K. Vrieze, Adv. Organomet. Chem., 21 (1982) 151.

7 K. Vrieze, J. Organomet. Chem., 300 (1986) 307.

8 M.P. García, A.M. López, M.A. Esteruelas, J.F. Lahoz and L.A. Oro, J. Chem. Soc. Chem. Commun., (1988) 793.

9 R.P. Hughes, G. Wilkinson, F.G.A. Stone and E.W. Abel (Eds.), Comprehensive Organometallic Chemistry, Pergamon, Oxford, 1982, Vol. 5, p. 288.

10 T. Yoshida, S. Otsuka, M. Matsumoto and K. Nakatsu, Inorg. Chim. Acta, 29 (1978) L257.

11 M. Iglesias, C. del Pino and S. Martínez-Carrera, J. Organomet. Chem., 317 (1986) 363.

12 M. Iglesias, C. del Pino, J.L. Nieto and S. Martínez-Carrera, Inorg. Chim. Acta, 145 (1988) 91.

13 W. Hieberg, O. Vohler and G. Braun, Z. Naturforsch. B, 13 (1958) 192.

14 T. Mitsudo, Y. Watanabe, H. Nakanishi, I. Morishima, T. Inubushi and T. Takegami, J. Chem. Soc. Dalton Trans., (1978) 1298.

15 N. Walker and D. Stuart, Acta Cryst. A, 39 (1983) 158.

16 J.M. Stewart, F.A. Kundell and J.C. Baldwing, The X-Ray 80 System version, Computer Science Center. University of Maryland, College Park, MD (U.S.A.), 1980.

17 M. Martínez-Ripoll and F.H. Cano, PESOS, Instituto de Química Física Rocasolano, C.S.I.C., Madrid, Spain, 1975.

18 PARST, M. Nardelli, Comput. Chem., 7 (1983) 95.

19 International Tables for X-Ray Crystallography, Vol. 4, Birmingham, Kynoch Press, 1974.